

Self-Aggregating Deep Cavitant Acts as a Fluorescence Displacement Sensor for Lysine Methylation

Yang Liu,[‡] Lizeth Perez,[†] Magi Mettry,[†] Connor J. Easley,[†] Richard J. Hooley,^{*,†} and Wenwan Zhong^{*,†,‡}

[†]Department of Chemistry and [‡]Environmental Toxicology Program, University of California-Riverside, Riverside, California 92521, United States

S Supporting Information

ABSTRACT: A dual-mode aggregative host:guest indicator displacement sensing system has been created for the detection of trimethylated peptides and determination of histone demethylase activity. The combination of selective recognition of suitably sized trimethylammonium salts and reversible lipophilic aggregation of the host:guest complex provides a unique quenching mechanism that is not only dependent on affinity for sensitivity but the lipophilicity of the indicator. In addition, aggregation can be controlled by the application of chaotropic anions in the mixture, allowing a second level of discrimination between hard lysine groups and softer trimethyllysines.

The diversity of proteins in living cells is greatly increased by post-translational modifications (PTMs).¹ Histone modifications such as methylation play important roles in regulation of gene transcription, strongly impacting cellular development, and they also respond to different stimulations leading to the development of pathological conditions.² Monitoring PTM changes in cells is essential in epigenetics and systems biology for better understanding of the regulation mechanisms of cellular processes³ and for the treatment of diseases associated with epigenetic disruption.⁴ Understanding how PTMs affect cell function and disease requires unambiguous detection of specific PTMs in complex mixtures, which remains a significant technical challenge, especially in a format amenable to automated high-throughput screening. Assays that employ antibodies,^{5a} commonly with radioisotope tagging,^{5b} are available to detect methylation on peptides, but few are able to discriminate between mono- and dimethylated or di- and trimethylated residues, or to differentiate between closely related PTM sites. Moreover, immunodetection methods are cumbersome, especially in a high-throughput environment.⁶

Synthetic receptors are an inviting solution to this problem, and there has been some elegant work recently published on the use of designed host molecules that bind to protein PTMs. The most notable targets are methylated lysine residues, which are substrates for simple receptors such as tetrasulfonatocalix[4]-arene (CX4)⁷ and cucurbit[7]uril (CB7)⁸ as well as more selective receptors designed either rationally⁹ or through dynamic combinatorial selection.¹⁰ The recognition of protein PTM targets often uses classical analytical techniques such as NMR and ITC: applications to sensing technologies require alternate readouts. The most common method for protein PTM sensing is indicator displacement assays,^{7,11,12} which mainly

exploit CX4 and CB7. These electron-rich cyclophanes and calixarenes cause charge-transfer induced quenching of the complexed fluorescent dyes. The analyte competes with the dye for binding to the cavity and restores the fluorescence. These displacement sensors have been used for enzyme assays, and sensor arrays have also been constructed using a group of cyclophane receptors for detection of histone peptides carrying variable methylations at various positions.^{7b} However, the dye-receptor interaction is shape- and functional group-dependent, which limits the choice of dyes in sensor construction and often requires specialized synthetic reporters. Here we describe a sensitive sensing system for peptide methylation and demethylase enzyme activity that functions with common, commercial fluorophores.

The host system used for this purpose is the self-folding, water-soluble deep cavitant **1** (Figure 1a). This is a versatile receptor, capable of selective recognition of a wide variety of substrates in aqueous,¹³ biomimetic membrane,¹⁴ and living cell^{14b} environments. Soft cations are the strongest guests, and binding affinities generally vary between mM and μ M, with R-NMe₃⁺ species such as acetylcholine showing the greatest affinity. As can be seen in

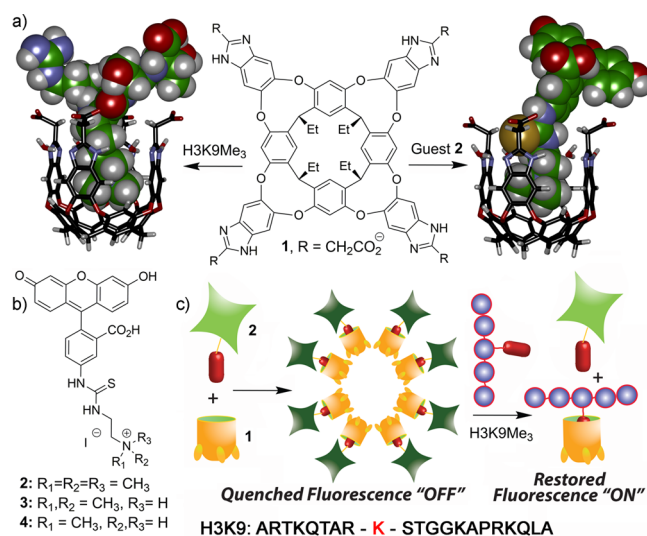


Figure 1. (a) Structure of host **1** and minimized models of the **1**·**2** and the **1**·(AR(KMe₃)ST) host:guest complexes (SPARTAN). (b) Fluorescent guests **2**–**4**. (c) Aggregation-based sensing system.

Received: June 8, 2016

Published: August 8, 2016

Figure 1, the cavity is filled by the $-\text{CH}_2\text{CH}_2\text{NMe}_3^+$ group (e.g., from trimethyllysine, KMe_3), with the remainder of the target structure positioned above the cavitand rim. Cavitand **1** is unique among water-soluble receptors in that its exterior is quite hydrophobic, as well as that of its internal cavity. This leads to some unusual assembly behavior upon the recognition of mildly lipophilic trimethylammonium-containing species: while **1** forms a simple 1:1 complex with small molecules such as choline, larger species that protrude out of the cavity can cause the receptor to aggregate into larger assemblies. This concept has been used by using **1** as sensing agent for acetylcholine, using the lowered relaxivity of a bound Gd-containing guest for MRI detection.¹⁵ This self-aggregation upon target binding introduces the possibility of a new strategy for indicator displacement assays. If fluorescence quenching of a bound dye can be effected upon aggregation, both the fluorophore and the binding anchor could be varied: as the fluorophore need not be inside the cavity, a far greater scope of reporters could be employed. In addition, the “binding handle” can be tailored to allow excellent specificity for desired targets.

Our initial tests were to determine a suitable fluorophore for the displacement assay. The requirements can be quite stringent: the binding of the indicator must be sufficiently robust as to be retained in a complex environment, but weaker than the binding of the selected target. The dye must be sufficiently lipophilic to confer aggregation, be quenched when bound (i.e., the fluorophores must be brought into close proximity upon aggregation), and turn on when released. In addition, long wavelength fluorescence is desirable for simple sensing, and water-solubility is essential. We tested a small range of water-soluble fluorescein-based dyes to determine their affinity and potential quenching range. Guests 2–4 were very simply synthesized in one or two steps from methylated ethylenediamine derivatives and commercial fluorescein isothiocyanate, and vary in their methylation state at the terminal nitrogen. NMe_3^+ species **2** is a well-established guest for **1** in lipid bilayer environments,¹⁴ and NHMe_2^+ dye **3**, NH_2Me^+ dye **4**, and fluorescein itself would be expected to have increasingly smaller affinities for **1**, due to mismatches in shape and charge-fitting with the cavity of **1**.

As can be seen from Figure 2, there is an obvious difference in behavior between the four dyes upon addition of increasing concentrations of cavitand **1** in phosphate buffered saline (PBS). While minimal changes in fluorescence were observed upon addition of **1** to fluorescein and NH_2Me^+ guest **4**, a slight decrease in fluorescence was observed for NMe_2H^+ guest **3**.

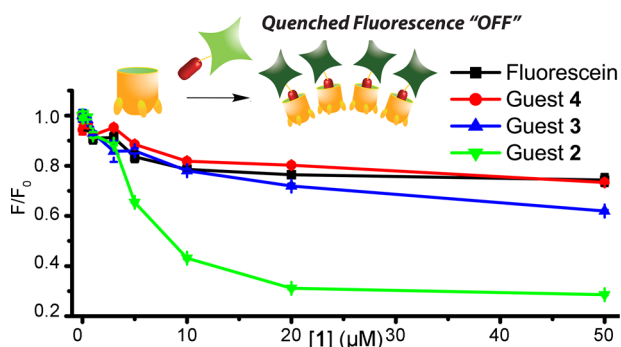


Figure 2. Aggregation-based quenching. Relative fluorescence of 2–4 at 3 μM with increasing [1] in PBS buffer (10 mM phosphate, 150 mM NaCl, pH 7.4).

However, when NMe_3^+ guest **2** was added, a strong loss in fluorescence was observed, reaching maximal quenching in the presence of 20 μM **1**, when only 30% of the original fluorescence was retained. The affinity of the various dyes was determined from these curves. The dissociation constant (K_d) of the 2:1 complex was estimated to be $17 \pm 10 \mu\text{M}$ by solving the complex dissociation equilibrium (see Supporting Information). The K_d values for NMe_2H^+ dye **3**, NH_2Me^+ dye **4**, and fluorescein were at least 10 times larger than that of **2**, indicating weak or nonspecific binding.

NMR analysis was consistent with the theory that the fluorescence loss observed upon addition of guest **2** to cavitand **1** was due to complexation-induced quenching via an aggregative mechanism.¹⁵ When **2** was titrated into a D_2O solution of **1**, proton signals for both **1** and **2** disappear and broaden out (see Supporting Information, Figure S2), indicating the formation of large, slowly tumbling aggregates. Large aggregates show a size-dependent decrease in T2 and the concomitant introduction of dipolar coupling effects that broaden ^1H NMR signals.¹⁶ In addition, new broad peaks appear, corresponding to expulsion of a THF molecule from the cavity of **1** (present in the cavity in the final isolation step¹³), illustrating that the host:guest recognition process occurs. Surface tension measurements (see Supporting Information) show a sharp reduction of the surface tension upon addition of **1** to a solution of **2**, something not observed upon increasing [1] or [2] alone. Evidently, upon association with **1** (even at μM concentrations), aggregation of the 1:2 complex occurs, positioning the fluorescein groups close to one another in the self-assembled (presumably micellar) aggregate, and self-quenching is observed. Indeed, greater quenching efficiency was obtained by increasing the concentration of the 1:2 complex while keeping the 1/2 ratio the same (see Supporting Information). By contrast, if the experiment was repeated in the presence of POPC vesicles, fluorescence recovery was observed (Figure S12). Cavitand **1** self-embeds into these vesicles very easily,^{14c} and this abrogates any self-association. The amount of **1** incorporated in a single vesicle is $<5\%$,^{14c} and no self-quenching of **2** can occur, corroborating the theory that the quenching of **2** upon binding in **1** is due to self-quenching between fluorophores upon aggregation of the 1:2 host:guest complex. The quenching should occur via a ground-state (i.e., static) mechanism, rather than via a dynamic mechanism such as diffusional collision.¹⁷ In fact, the flattening of the Stern–Volmer plot of F_0/F vs [1] at high [1] indicated the presence of both free and bound **2** in the system. The quenching phenomenon was inversely related to temperature, with less quenching observed at higher temperature. Fluorescence lifetime measurements also showed that no change in the lifetime of **2** occurred when mixed with cavitand **1**, even at the optimal concentration ratio where $F/F_0 = 0.3$. All these experiments support the notion of static quenching.

This aggregation-based quenching mechanism is unique and distinctly different from the standard indicator displacement assays that occur solely via host:guest quenching interactions.¹² This process is controlled by both the highly selective host behavior and self-aggregative properties of **1**. Only a selected few guests cause this aggregation: purely hydrophobic species (e.g., hydrocarbons) do not, nor do small charged species such as choline.¹³ Only mildly lipophilic R-NMe_3^+ guests such as **2** have been shown to cause this aggregation.¹⁵ As such, this phenomenon can be exploited to establish simple, homogeneous in-solution displacement assays for the detection of suitable substrates, if the substrate is a sufficiently good guest to displace

the indicator **2**. As the measured K_d of **2** was $\sim 17 \mu\text{M}$, only strongly binding targets should be capable of this displacement, allowing the formation of a selective sensor.

As NMe_3^+ -based substrates are the most strongly bound by **1**, we envisaged that this system would be an excellent candidate for the detection of lysine methylation PTMs. The specific, strong affinity of **2** for the host would ensure selective detection of trimethylated targets. Our initial tests involved the fluorescence detection of trimethylation on histone H3 peptide fragments. The primary amino acid sequence of the H3 peptides used (amino acids 1–21) is shown in Figure 1. We initially focused on variably methylated peptides at the lysine 9 position. The sensor was constructed by mixing cavitand **1** and guest **2** at an optimized ratio of 6:1 in PBS, with $[\mathbf{2}] = 3 \mu\text{M}$. Three H3 peptide fragments with methylations on K9 (from zero to three methyl groups: H3, H3K9Me, and H3K9Me₃) were titrated into the system, and the fluorescence recovery analyzed with respect to peptide concentration (see Figure 3).

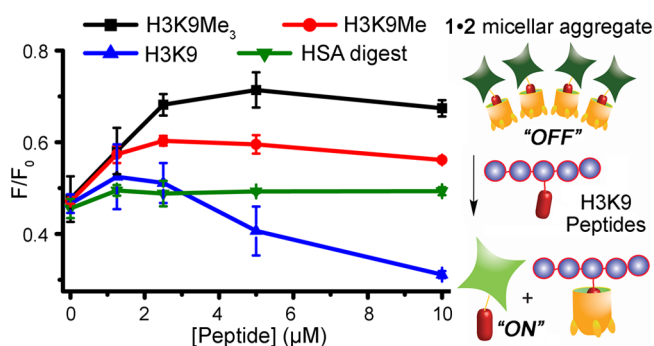


Figure 3. Fluorescence recovery induced by mixing modified (H3K9Me, H3K9Me₃) or unmodified (H3K9) histone peptides (H3, 1–21), or the protease digest of human serum albumin (HSA) with the sensor system (PBS buffer, 20 μM **1**, 3 μM **2**).

Gratifyingly, addition of the trimethylated peptide (H3K9Me₃) caused a significant recovery of the fluorescence signal upon addition of only 2 μM peptide. The fluorescence recovery reached a maximum at 5 μM peptide, and this effect was selective for the trimethylated NMe_3^+ guest, as would be expected from the previous affinity measurements. If the monomethylated peptide (H3K9Me) was added, some fluorescence recovery was observed, but to a far lower extent than for H3K9Me₃. In addition, the parent unmethylated peptide (H3K9) caused no recovery of the fluorescence signal within the initial concentration range of 0 to 5 μM . This indicator displacement assay is selective and quite robust in systems that mimic cell extraction: for example, the addition of the protease digest from human serum albumin (HSA digest, Figure 3) did not change the fluorescence of the sensor. Also, addition of a trypsin-digested cell lysate from mouse macrophages did not alter the response curve produced by H3K9Me₃ (see Supporting Information).

The indicator displacement did show an unusual outcome at higher peptide concentrations, most strongly observed for the unmethylated H3K9. If the concentration of H3K9 was higher than 5 μM , the observed fluorescence *decreased* significantly (blue curve, Figure 3). We speculated that this excess quenching could be the result of aggregation mediated by the electrostatic interaction between the cationic histone peptide and the anionic **1·2** complex. If true, the aggregation effect should be affected by the both salt concentration and type, i.e., show Hofmeister

dependence. The Hofmeister series is well-established for its effects on protein solubility, but only recently has its effects on cavity-based molecular recognition been investigated.¹⁸ We tested the effect on fluorescence quenching induced by the combination of **1**, **2**, and H3K9 in the presence of both “salting-in” (chaotropic) and “salting out” (kosmotropic) anions (Figure 4). A series of solutions were prepared by increasing $[\text{NaCl}]$ from

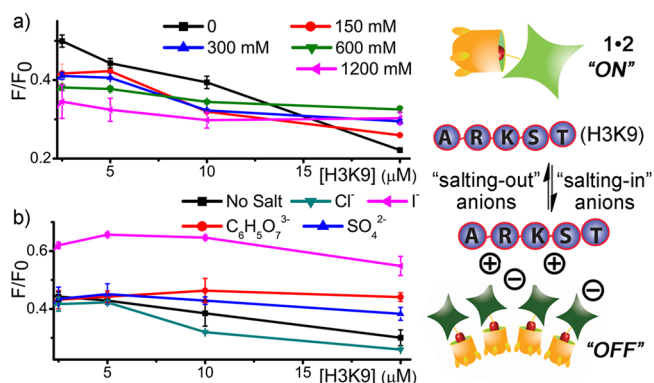


Figure 4. Hofmeister-dependent aggregation. Effect of varying (a) $[\text{NaCl}]$ and (b) anion type with $[\text{X}^-] = 150 \text{ mM}$ on the fluorescence of the sensor (18 μM **1**, 3 μM **2**).

0 to 1200 mM in 10 mM sodium phosphate (pH 7.4) or by fixing $[\text{NaCl}] = 150 \text{ mM}$ but varying the type of anion in the phosphate buffer. The sensor was constructed by mixing 3 μM guest **2** and 18 μM cavitand **1**, and the fluorescence was monitored with respect to $[\text{H3K9}]$. The initial observation was that the quenching process could be abrogated upon increasing $[\text{NaCl}]$ (Figure 4a). As expected, increasing the ionic strength of the system reduced electrostatic interactions between the cationic peptide and the **1·2** complex. Salt concentration has been shown to disrupt the recognition of cationic proteins with **1** in membrane bilayers,¹⁹ so this result was somewhat expected. The most interesting observation was in the presence of “salting-out” salts such as citrate, lowered fluorescence decrease is observed, corresponding to a lowered amount of aggregation with the cationic H3K9. This makes sense: as chaotropes make water more “water-like”, increased binding of sodium ions to the external anionic carboxylates is observed, thereby reducing the net charge on the host (as has been shown by Gibb with his anionic host^{18b}) and reducing the electrostatic attraction between **1** and H3K9. Whereas the addition of 150 mM citrate completely removes any fluorescence loss due to aggregation (red line, Figure 4b), sulfate (a weaker chaotrope) has a smaller effect (blue line), yet is still more effective than adding no salt at all. The slightly chaotropic chloride is the least effective additive. Most interestingly, addition of iodide *increases* the baseline fluorescence significantly (something not observed for the other salts). The most likely explanation is that the soft iodide anion has some affinity for the cavity itself,^{18b} and competitively displaces **2**, regenerating the fluorescence.

Interestingly, the electrostatically induced aggregation at higher peptide concentration was not significant with the trimethylated peptide H3K9Me₃, presumably due to the replacement of hard NH_3^+ ions with the softer, less H-bonding NMe_3^+ . This leads to a large signal difference between the unmethylated and trimethylated peptides, in either no salt or PBS buffered condition ($[\text{NaCl}] \leq 150 \text{ mM}$), adding a second dimension to the sensing process *other than merely target affinity*.

This feature makes our sensor ideal for monitoring enzymatic changes in peptide methylation-catalyzed histone-lysine *N*-methyltransferase or lysine demethylases. Known assays often rely on coupled chemical or enzyme reactions for signaling or require target immobilization and separation.²⁰ As our sensor can clearly differentiate between trimethylated, monomethylated, and nonmethylated H3 peptides, it can directly monitor the methylation or demethylation processes in solution. The sensor was employed to monitor the reactivity of histone demethylase JMJD2E, which catalyzes the demethylation of histone H3 at lysine residue 9. Figure S11a shows the fluorescence trace of the demethylation assay. Upon mixing 10 μM H3K9Me₃ with the 1-2 sensor (20 μM 1, 3 μM 2), the trimethylated peptide displaced the guest from the host, conferring fluorescence recovery on the system. The addition of 100 nM JMJD2E and its cofactors (1.5 mM ascorbate, 10 μM Fe²⁺, and 50 μM 2-oxoglutarate) initiated the demethylation reaction. The observed fluorescence continuously decreased over time, as the demethylated products (either H3K9Me₂ or H3K9Me) have much lower affinity for 1 and are incapable of displacing 2. The fluorescence decrease plateaued at 50 min, after which no more demethylated product was generated. A control experiment showed that when the ratio of H3K9Me₃ and H3K9 was varied while keeping [peptide] = 20 μM , the fluorescence increased linearly with increasing fraction of H3K9Me₃ (Figure S11b). This indicates that the sensor can monitor changes in [H3K9Me₃] or [H3K9] during enzyme assays, and so we applied it to quantitate the effect of varying [JMJD2E] on demethylation of 20 μM H3K9Me₃ (Figure S11c) and tested the impact on enzyme activity from 2,4-dicarboxypyridine (2,4-PDCA), a 2-oxoglutarate analogue and known inhibitor of JMJD2E (Figure S11d).²¹ Higher sensor fluorescence was observed upon increasing [2,4-PDCA] (Figure S11d), fixing [JMJD2E] at 800 nM and $t = 30$ min. The IC₅₀ value was 7.4 μM , close to the literature value of ~ 3 μM .

In conclusion, we have established a dual-mode aggregative indicator displacement sensing system for the detection of trimethylated peptides and determination of histone demethylase activity. The combination of selective recognition of suitably sized NMe₃⁺ salts and the targeted, reversible lipophilic aggregation of the host:guest complex provides a unique quenching mechanism that is not only dependent on affinity for sensitivity but the lipophilicity of the host:guest sensor. In addition, aggregation can be controlled by the application of chaotropic anions in the analysis mixture, allowing a second level of discrimination between hard lysine groups and softer trimethyllysines. The aggregation-induced quenching mechanism gives higher flexibility in the selection of the signaling units, which are no longer limited to target-complementary dyes.

■ ASSOCIATED CONTENT

Supporting Information

The Supporting Information is available free of charge on the ACS Publications website at DOI: 10.1021/jacs.6b05897.

Characterization and spectral data (PDF)

■ AUTHOR INFORMATION

Corresponding Authors

*richard.hooley@ucr.edu

*wenwan.zhong@ucr.edu

Notes

The authors declare no competing financial interest.

■ ACKNOWLEDGMENTS

The authors would like to thank the National Science Foundation (CHE-1151773 to R.J.H. and CHE-1057113 to W.Z.) for support.

■ REFERENCES

- (1) Davidson, V. L. *Biochemistry* **2007**, *46*, 5283–5292.
- (2) Waldmann, T.; Schneider, R. *Curr. Opin. Cell Biol.* **2013**, *25*, 184–189.
- (3) Lee, S. *Toxicol. Res.* **2013**, *29*, 81–86.
- (4) Walsh, C. T.; Garneau-Tsodikova, S.; Gatto, G. J., Jr. *Angew. Chem., Int. Ed.* **2005**, *44*, 7342–7372.
- (5) (a) Carlson, S. M.; Moore, K. E.; Green, E. M.; Martin, G. M.; Gozani, O. *Nat. Protoc.* **2014**, *9*, 37–50. (b) Horiuchi, K. Y.; Eason, M. M.; Ferry, J. J.; Planck, J. L.; Walsh, C. P.; Smith, R. F.; Howitz, K. T.; Ma, H. *Assay Drug Dev. Technol.* **2013**, *11*, 227–236.
- (6) Hattori, T.; Taft, J. M.; Swist, K. M.; Luo, H.; Witt, H.; Slattery, M.; Koide, A.; Ruthenburg, A. J.; Krajewski, K.; Strahl, B. D.; White, K. P.; Farnham, P. J.; Zhao, Y.; Koide, S. *Nat. Methods* **2013**, *10*, 992–995.
- (7) (a) Norouzy, A.; Azizi, Z.; Nau, W. M. *Angew. Chem., Int. Ed.* **2015**, *54*, 792–795. (b) Minaker, S. A.; Daze, K. D.; Ma, M. C. F.; Hof, F. *J. Am. Chem. Soc.* **2012**, *134*, 11674–11680.
- (8) Gamal-Eldin, M. A.; Macartney, D. H. *Org. Biomol. Chem.* **2013**, *11*, 1234–1241.
- (9) (a) Shaurya, A.; Dubicki, K. I.; Hof, F. *Supramol. Chem.* **2014**, *26*, 583–590. (b) Daze, K. D.; Hof, F. *Acc. Chem. Res.* **2013**, *46*, 937–945. (c) Daze, K. D.; Pinter, T.; Beshara, C. S.; Ibraheem, A.; Minaker, S. A.; Ma, M. C.; Courtemanche, R. J.; Campbell, R. E.; Hof, F. *Chem. Sci.* **2012**, *3*, 2695–2699.
- (10) Ingerman, L. A.; Cuellar, M. E.; Waters, M. L. *Chem. Commun.* **2010**, *46*, 1839–1841.
- (11) Ghale, G.; Nau, W. M. *Acc. Chem. Res.* **2014**, *47*, 2150–2159.
- (12) Biedermann, F.; Hathazi, D.; Nau, W. M. *Chem. Commun.* **2015**, *51*, 4977–4980.
- (13) Biros, S. M.; Ullrich, E. C.; Hof, F.; Trembleau, L.; Rebek, J., Jr. *J. Am. Chem. Soc.* **2004**, *126*, 2870–2876.
- (14) (a) Liu, Y.; Liao, P.; Cheng, Q.; Hooley, R. J. *J. Am. Chem. Soc.* **2010**, *132*, 10383. (b) Ghang, Y.-J.; Schramm, M. P.; Zhang, F.; Acey, R. A.; David, C. N.; Wilson, E. H.; Wang, Y.; Cheng, Q.; Hooley, R. J. *J. Am. Chem. Soc.* **2013**, *135*, 7090–7093. (c) Ghang, Y.-J.; Lloyd, J. J.; Moehlig, M. P.; Arguelles, J. K.; Mettry, M.; Zhang, X.; Julian, R. R.; Cheng, Q.; Hooley, R. J. *Langmuir* **2014**, *30*, 10161–10166.
- (15) Li, V.; Ghang, Y.-J.; Hooley, R. J.; Williams, T. J. *Chem. Commun.* **2014**, *50*, 1375–1377.
- (16) Cala, O.; Dufourc, E. J.; Fouquet, E.; Manigand, C.; Laguerre, M.; Pianet, I. *Langmuir* **2012**, *28*, 17410–17418.
- (17) Lakowicz, J. R. *Principles of Fluorescence Spectroscopy*; Springer US: Boston, MA, 2006; pp 277–330.
- (18) (a) Gibb, C. L. D.; Gibb, B. C. *J. Am. Chem. Soc.* **2011**, *133*, 7344–7347. (b) Carnegie, R. S.; Gibb, C. L.; Gibb, B. C. *Angew. Chem., Int. Ed.* **2014**, *53*, 11498–11500.
- (19) Ghang, Y.-J.; Perez, L.; Morgan, M. A.; Si, F.; Hamdy, O. M.; Beecher, C. N.; Larive, C. K.; Julian, R. R.; Zhong, W.; Cheng, Q.; Hooley, R. J. *Soft Matter* **2014**, *10*, 9651–9656.
- (20) (a) Kawamura, A.; Tumber, A.; Rose, N. R.; King, O. N. F.; Daniel, M.; Oppermann, U.; Heightman, T. D.; Schofield, C. J. *Anal. Biochem.* **2010**, *404*, 86–93. (b) Xu, W.; Podoll, J. D.; Dong, X.; Tumber, A.; Oppermann, U.; Wang, X. *J. Med. Chem.* **2013**, *56*, 5198–5202.
- (21) (a) Tsukada, Y.-I.; Fang, J.; Erdjument-Bromage, H.; Warren, M. E.; Borchers, C. H.; Tempst, P.; Zhang, Y. *Nature* **2006**, *439*, 811–816. (b) Kaniskan, H. Ü.; Konze, K. D.; Jin, J. *J. Med. Chem.* **2015**, *58*, 1596–1629.